Stem Cell Reports
Article

ISSCR

OPEN ACCESS

# Activin Is Superior to BMP7 for Efficient Maintenance of Human iPSC-Derived Nephron Progenitors

Shunsuke Tanigawa,[1] Hidekazu Naganuma,[1,2] Yusuke Kaku,[1] Takumi Era,[3] Tetsushi Sakuma,[4] Takashi Yamamoto,[4] Atsuhiro Taguchi,[1,5] and Ryuichi Nishinakamura[1,*]

[1]Department of Kidney Development, Institute of Molecular Embryology and Genetics, Kumamoto University, Kumamoto 860-0811, Japan
[2]Department of Urology, Kyushu University Graduate School of Medical Science, Fukuoka 812-8582, Japan
[3]Department of Cell Modulation, Institute of Molecular Embryology and Genetics, Kumamoto University, Kumamoto 860-0811, Japan
[4]Department of Mathematical and Life Sciences, Graduate School of Science, Hiroshima University, Hiroshima 739-8526, Japan
[5]Present address: Department of Genome Regulation, Max Planck Institute for Molecular Genetics, 14195 Berlin, Germany
*Correspondence: ryuichi@kumamoto-u.ac.jp
https://doi.org/10.1016/j.stemcr.2019.07.003

## SUMMARY

Kidney formation is regulated by the balance between maintenance and differentiation of nephron progenitor cells (NPCs). Now that directed differentiation of NPCs from human induced pluripotent stem cells (iPSCs) can be achieved, maintenance and propagation of NPCs *in vitro* should be beneficial for regenerative medicine. Although WNT and FGF signals were previously shown to be essential for NPC propagation, the requirement for BMP/TGFβ signaling remains controversial. Here we reveal that activin has superior effects to BMP7 on maintenance efficiency of human iPSC-derived NPCs. Activin expanded ITGA8$^+$/PDGFRA$^-$/SIX2-GFP$^+$ NPCs by 5-fold per week at 80%–90% efficiency, and the propagated cells possessed robust capacity for nephron formation both *in vitro* and *in vivo*. The expanded cells also maintained their nephron-forming potential after freezing. Furthermore, the protocol was applicable to multiple non-GFP-tagged iPSC lines. Thus, our activin-based protocol will be applicable to a variety of research fields including disease modeling and drug screening.

## INTRODUCTION

The kidney contains a large number of nephrons, which are functional units consisting of glomeruli and renal tubules. The kidney develops by interactions between the metanephric mesenchyme and the ureteric bud, the former of which contains nephron progenitor cells (NPCs) that form the epithelia of glomeruli and renal tubules in response to wingless-type mouse mammary tumor virus integration site family member (WNT) signals emitted from the latter. At the same time, the ureteric bud-derived signals maintain and propagate some NPCs in the undifferentiated state, and the balance between NPC maintenance/propagation and differentiation is critical for kidney development (Costantini and Kopan, 2010). NPCs cease propagation and become terminally differentiated within a few days after birth in mice (Hartman et al., 2007) and at approximately 36 weeks of gestation in humans (Lindstrom et al., 2018a).

In recent years, we and others have succeeded in NPC induction and resultant kidney organoid generation from mouse embryonic stem cells (ESCs) and/or human induced pluripotent stem cells (iPSCs) (Morizane et al., 2015; Taguchi et al., 2014; Taguchi and Nishinakamura, 2017; Takasato et al., 2016). Thus, NPC purification and expansion should have an impact on regenerative medicine targeting cell therapy, disease modeling, drug screening, and transplantable kidney reconstruction, because large numbers of NPCs are required to achieve these goals. Indeed, several groups, including ours, have reported expansion protocols for NPCs derived from ESCs or iPSCs (Brown et al., 2015; Li et al., 2016; Tanigawa et al., 2015, 2016), all of which involved fibroblast growth factor (FGF) and WNT signals, consistent with previous findings *in vivo* (Barak et al., 2012). However, the utilization of bone morphogenetic protein (BMP) signaling molecules and their inhibitors differed depending on the protocol. Brown et al. (2015) reported expansion of human iPSC-derived NPCs by addition of BMP7 and BMP receptor inhibitor LDN193189. However, their NPCs only formed renal tubule-like structures and not glomeruli. When the same protocol was applied to NPCs from human embryos, some NPC genes were maintained, but the expanded cells failed to show nephron formation histologically (Pode-Shakked et al., 2017). We reported expansion of NPCs from mouse embryos by adding leukemia inhibitory factor (LIF) and low concentrations of BMP7. This protocol was applicable to NPCs derived from mouse ESCs and human iPSCs, and generated both glomeruli and renal tubules, emphasizing that the full potency for nephron formation was maintained in the expanded NPCs. However, the expansion period for human iPSC-derived NPCs was limited (1–2 weeks). Subsequently, Li et al. (2016) reported long-term expansion of NPCs from mouse and human embryos. They utilized a spheroid culture in the presence of LIF, BMP7, and combination of BMP and transforming growth factor β (TGFβ) receptor inhibitors, and obtained propagation of human

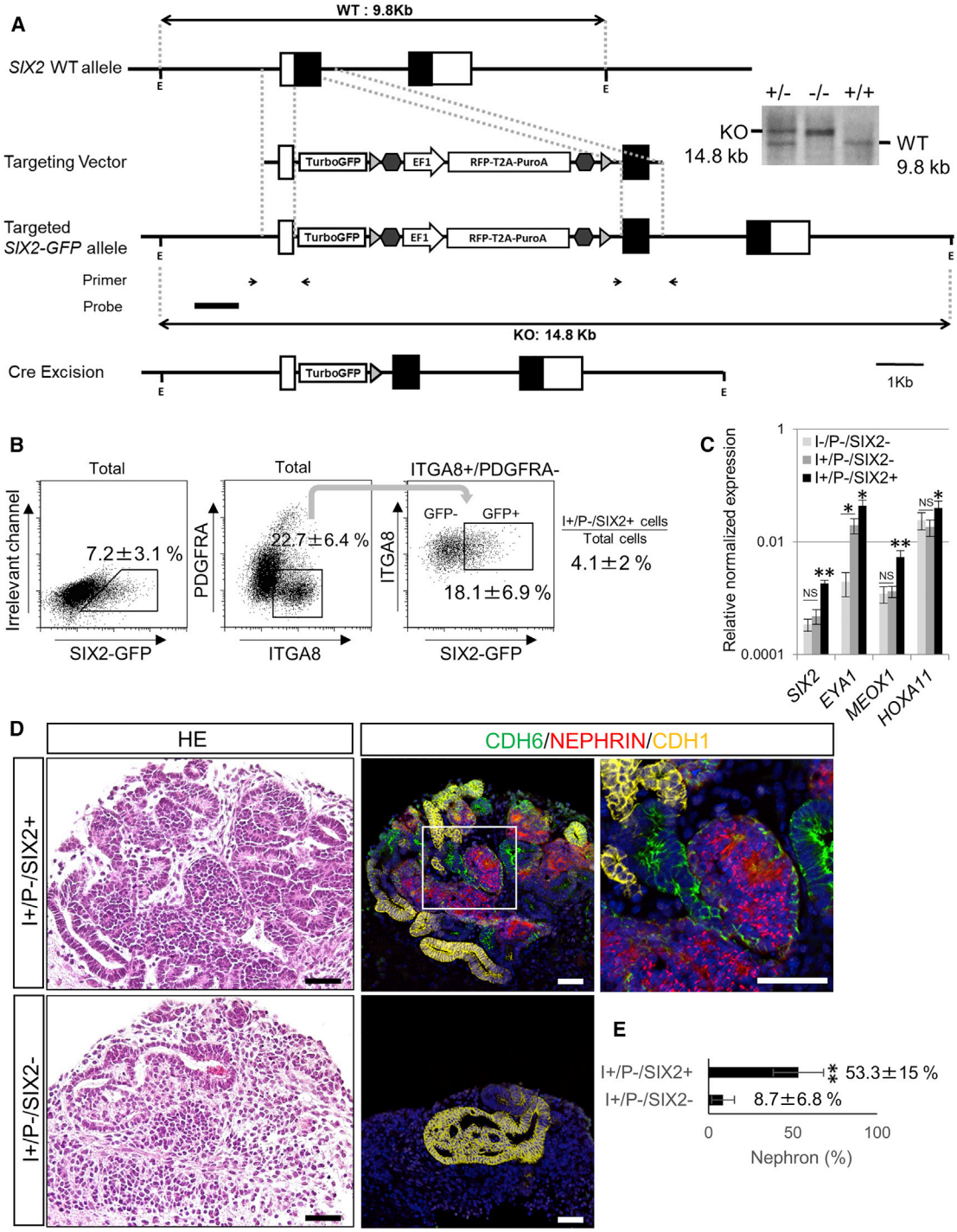


**Figure 1. NPCs Are Enriched in the ITGA8$^+$/PDGFRA$^-$/SIX2-GFP$^+$ Fraction in Human iPSC-Derived Kidney Tissues**

(A) Generation of SIX2-GFP iPSCs by TALENs. A GFP cassette was inserted into exon 1 in the *SIX2* gene by homologous recombination. The selection cassette was removed by Cre-mediated excision. Southern blot analysis of wild-type (WT) (+/+), heterozygous (+/−), and homozygous (−/−) clones (right). The positions of the probe for Southern blotting and PCR primers are indicated on the map (left).

(B) Isolation of nephron progenitors from the ITGA8$^+$/PDGFRA$^-$/SIX2-GFP$^+$ fraction in induced NPCs. The gates in the dot plots show SIX2-GFP$^+$ cells in the total cells (left), ITGA8$^+$/PDGFRA$^-$ cells in the total cells (center), and ITGA8$^+$/SIX2-GFP$^+$ cells in the ITGA8$^+$/PDGFRA$^-$ fraction (right). I, ITGA8; P, PDGFRA; SIX2+, SIX2-GFP$^+$. The percentage of ITGA8$^+$/PDGFRA$^-$/SIX2-GFP$^+$ cells in the total cells is shown on the right (I+/P−/SIX2+ cells/total cells). Data represent means ± SEM from six independent experiments.

*(legend continued on next page)*

embryo-derived NPCs for 7 months. They further claimed that the same protocol was applicable to human iPSC-derived NPCs. However, none of these reports addressed the quantitative percentages of human NPCs. If NPCs constitute only a minor population of the expanded cells, nephrogenesis will occur in limited areas of the tissues, and thus hamper reproducible disease modeling or drug screening. Thus, it is necessary to establish methods that can measure the precise percentages of functional NPCs in expanded cells.

The transcription factor SIX2 is specifically expressed in NPCs and antagonizes their Wnt-mediated differentiation (Kobayashi et al., 2008). Li et al. (2016) generated SIX2-GFP iPSCs, but did not perform quantitative analysis of GFP$^+$ NPCs. Meanwhile, we reported that NPCs from mouse embryos and human iPSCs could be sorted as an ITGA8$^+$/PDGFRA$^-$ population (Kaku et al., 2017; Taguchi et al., 2014). ITGA8 was expressed in NPCs from both mice and humans *in vivo* (O'Brien et al., 2016), and deletion of *Itga8*, as well as its ligand nephronectin, led to kidney hypoplasia in mice (Muller et al., 1997), indicating that ITGA8 expression in NPCs is critical for kidney development. Single-cell RNA-sequencing (RNA-seq) analysis of nephron progenitors in human embryos further revealed that they were ITGA8$^+$/PDGFRA$^-$ (Lindstrom et al., 2018b; O'Brien et al., 2016). Therefore, we reasoned that the combination of these two criteria (SIX2-GFP$^+$ and ITGA8$^+$/PDGFRA$^-$) would lead to more reliable and quantitative readouts for measurement of maintenance efficiency of NPCs upon culture. For this purpose, we generated SIX2-GFP human iPSCs and measured the percentages of ITGA8$^+$/PDGFRA$^-$/SIX2-GFP$^+$ NPCs, leading to the unexpected finding that activin A (activin) has superior effects to BMP7 on the maintenance efficiency of human iPSC-derived NPCs.

## RESULTS

### Human iPSC-Derived NPCs Are Enriched in the ITGA8$^+$/PDGFRA$^-$/SIX2-GFP$^+$ Fraction

To isolate NPCs, we inserted GFP into the *SIX2* locus of human iPSCs by homologous recombination. We constructed a pair of plasmids expressing TALENs that targeted regions in close proximity to the *SIX2* start codon, and introduced these plasmids together with a targeting vector containing the *GFP* gene and homology arms into iPSCs (Figure 1A). We successfully obtained heterozygous *GFP*-knockin clones and induced them toward NPCs, based on our previously published protocol (Taguchi et al., 2014; Taguchi and Nishinakamura, 2017). At day 13, SIX2-GFP$^+$ cells constituted 7.2% of the induced tissues (n = 6; Figure 1B). Meanwhile, the ITGA8$^+$/PDGFRA$^-$ population represented 22.7%, and 18.1% of these cells were SIX2-GFP$^+$. Thus, 4.1% of the total cells were ITGA8$^+$/PDGFRA$^-$/SIX2-GFP$^+$. Expression of NPC marker *Eya1* in ITGA8$^+$/PDGFRA$^-$/SIX2-GFP$^+$ or ITGA8$^+$/PDGFRA$^-$/SIX2-GFP$^-$ cells was higher than that in ITGA8$^-$/PDGFRA$^-$/SIX2-GFP$^-$ cells, while the expression levels of other NPC markers, such as *SIX2*, *MEOX1*, and *HOXA11*, were higher in ITGA8$^+$/PDGFRA$^-$/SIX2-GFP$^+$ cells even when compared with ITGA8$^+$/PDGFRA$^-$/SIX2-GFP$^-$ cells (Figure 1C). When these fractions were aggregated and combined with embryonic spinal cord, a classical inducer of nephrogenesis, ITGA8$^+$/PDGFRA$^-$/SIX2-GFP$^+$ cells formed nephron epithelia of glomeruli and renal tubules (CADHERIN6 [CDH6]: proximal tubules; NEPHRIN: podocytes; E-CADHERIN [CDH1]: distal tubules) that constituted 53.3% of the induced kidney tissues (Figures 1D and 1E). In contrast, ITGA8$^+$/PDGFRA$^-$/SIX2-GFP$^-$ cells exhibited minimal nephrogenesis (8.7% of the whole tissues). The ITGA8$^-$/PDGFRA$^-$/SIX2-GFP$^-$ fraction also showed minimal nephrogenesis (Figure S1), consistent with our previous report (Kaku et al., 2017). Thus, human iPSC-derived NPCs were preferentially populated in the ITGA8$^+$/PDGFRA$^-$/SIX2-GFP$^+$ fraction.

### BMP7 Is Insufficient to Maintain Human iPSC-Derived NPCs

To propagate iPSC-derived ITGA8$^+$/PDGFRA$^-$/SIX2-GFP$^+$ cells, we aggregated the sorted cells and cultured them as spheres for 7 days under our previously defined conditions, which included FGF9, CHIR99021 (CHIR), LIF, DAPT (N-[N-(3,5-difluorophenacetyl)-L-alanyl]-S-phenylglycine

(C) Progenitor marker expression in each progenitor fraction. Isolated cells from the indicated fractions were analyzed for gene expression by qPCR. Data represent means ± SEM from three independent experiments. *p < 0.05, **p < 0.01 versus ITGA8$^-$/PDGFRA$^-$/SIX2-GFP$^-$; NS, not significant.

(D) Histology and immunostaining of spinal cord-induced tissues from isolated NPCs at day 9 after induction. Magnified images of the ITGA8$^+$/PDGFRA$^-$/SIX2-GFP$^+$ fraction are shown on the right. CDH6 (green) shows proximal tubules, NEPHRIN (red) shows glomeruli, and CDH1 (yellow) shows distal tubules. Scale bars: 200 μm (left and middle) and 50 μm (right).

(E) Quantification of nephron areas in induced tissues. The percentages of nephron structures in the induced tissues relative to the total section areas were calculated and shown as bar graphs. **p < 0.01 versus ITGA8$^+$/PDGFRA$^-$/SIX2-GFP$^-$ (n = 3 per group).

See also Figure S1.

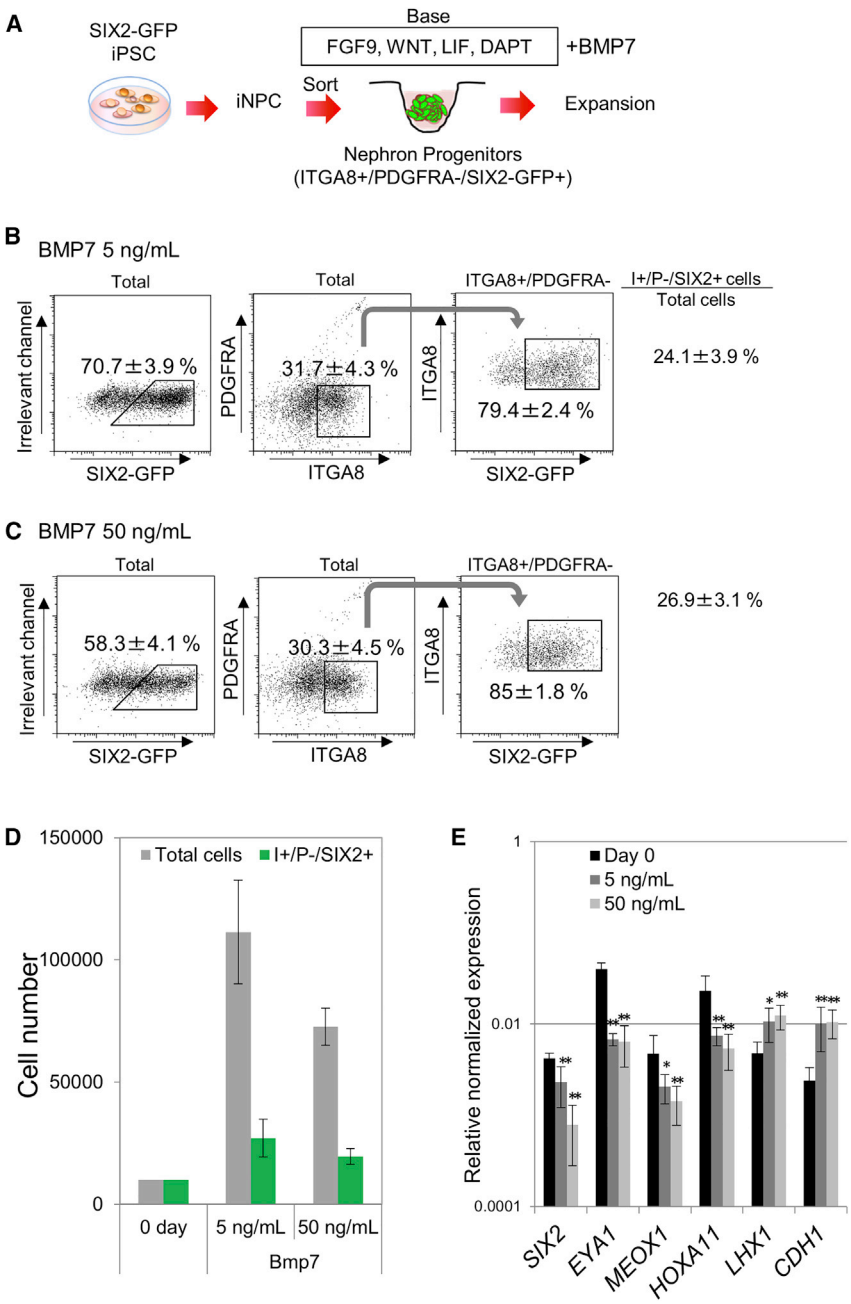


**Figure 2. BMP7 Is Insufficient to Maintain Human iPSC-Derived NPCs**

(A) Schematic diagram of the culture procedure for purified NPCs. Purified NPCs were aggregated and cultured in basal medium containing FGF9, CHIR, LIF, DAPT, and BMP7 (5 or 50 ng/mL) for 7 days.

(B) Flow-cytometry quantification of ITGA8$^+$/PDGFRA$^-$/SIX2-GFP$^+$ (I+/P−/SIX2+) cells after culture with BMP7 (5 ng/mL) for 7 days. The percentage of ITGA8$^+$/PDGFRA$^-$/SIX2-GFP$^+$ cells in the total cells is shown on the right (I+/P−/SIX2+ cells/total cells). n = 3 per group.

(C) Flow-cytometry quantification of ITGA8$^+$/PDGFRA$^-$/SIX2-GFP$^+$ cells after culture with BMP7 (50 ng/mL) for 7 days (n = 3 per group).

(D) Numbers of total and ITGA8$^+$/PDGFRA$^-$/SIX2-GFP$^+$ cells after 7 days of culture (n = 3 per group).

(E) qPCR analysis of progenitor markers in NPCs after culture for 7 days. Freshly isolated ITGA8$^+$/PDGFRA$^-$/SIX2-GFP$^+$ cells were used as a positive control (Day 0). Data represent means ± SEM from three independent experiments. *p < 0.05, **p < 0.01, cells cultured with BMP7 versus Day 0.

See also Figure S2.

t-butyl ester), and BMP7 (Figure 2A) (Tanigawa et al., 2016). We previously proposed that a relatively low concentration of BMP7 (5 ng/mL) was beneficial for maintenance of NPCs, while other reports utilized higher concentrations (30–50 ng/mL) along with BMP receptor inhibitors (Barak et al., 2012; Brown et al., 2015; Li et al., 2016). Thus, we examined the effects of two concentrations of BMP7 (5 ng/mL versus 50 ng/mL). However, the percentages of SIX2-GFP$^+$ cells were 70.7% and 58.3%, respectively, and ITGA8$^+$/PDGFRA$^-$/SIX2-GFP$^+$ cells constituted only 24.1% and 26.9% of the total cells, respectively (Figures 2B and 2C). Although the cell numbers increased significantly during the 7-day culture, the expansion of the ITGA8$^+$/SIX2-GFP$^+$ fraction was only 2.7-fold and 1.9-fold, respectively (Figure 2D). Consistent with these observations, the expression levels of NPC markers in the whole spheres decreased while those of differentiation markers (*LHX1*, *CDH1*) increased (Figure 2E). Thus, BMP7-based conditions were insufficient for maintenance of ITGA8$^+$/PDGFRA$^-$/SIX2-GFP$^+$ NPCs *in vitro*, although the lower

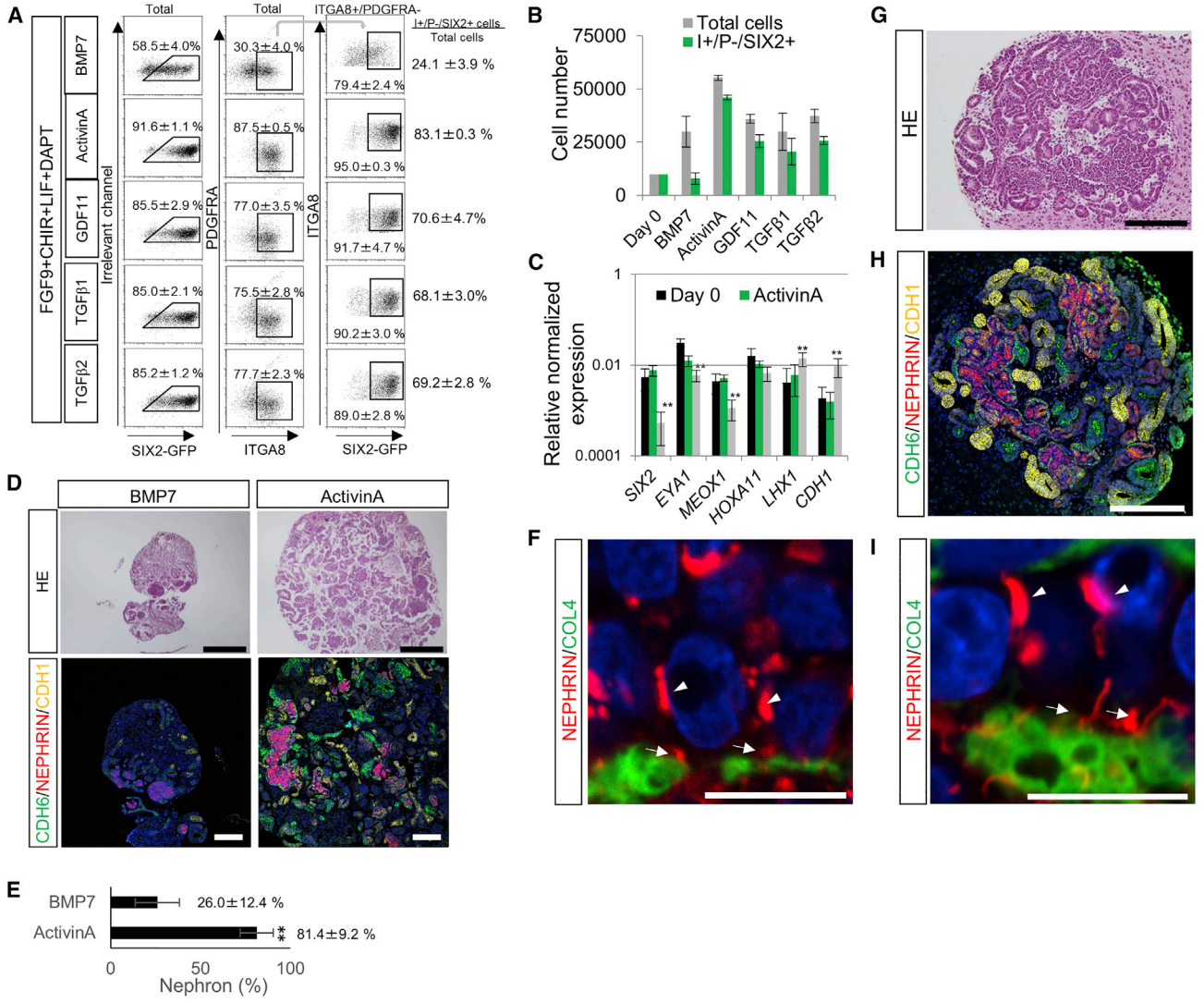


**Figure 3. Activin Maintains NPCs at High Efficiency**

(A) Quantification of ITGA8$^+$/PDGFRA$^-$/SIX2-GFP$^+$ (I+/P−/SIX2+) cells cultured for 7 days with BMP7 or TGFβ-related ligands. NPCs were cultured for 7 days in basal medium (as shown in Figure 2A) with addition of BMP7 (50 ng/mL) or TGFβ-related ligands activin (50 ng/mL), GDF11 (50 ng/mL), TGFβ1 (50 ng/mL), or TGFβ2 (50 ng/mL), then analyzed by flow cytometry. The percentage of ITGA8$^+$/PDGFRA$^-$/SIX2-GFP$^+$ cells in the total cells is shown on the right (I+/P−/SIX2+ cells/total cells). n = 3 per group.

(B) Numbers of total and ITGA8$^+$/PDGFRA$^-$/SIX2-GFP$^+$ cells after culture for 7 days (n = 3 per group).

(C) qPCR analysis of NPC markers. Freshly isolated ITGA8$^+$/PDGFRA$^-$/SIX2-GFP$^+$ cells were used as a positive control (Day 0). Data represent means ± SEM from three independent experiments. **p < 0.01 versus day 0.

(D) Reconstitution of three-dimensional nephron structures by NPCs cultured with BMP7 or activin for 7 days. H&E-stained images (upper) and immunostained images (lower) of induced nephrons from NPCs cultured with BMP7 or activin are shown. Scale bars, 200 μm.

(E) Quantification of nephron areas in induced tissues. The percentages of nephron-like structures in the induced tissues related the total section areas were calculated and shown as bar graphs. Data represent means ± SEM from three independent experiments. **p < 0.01, cells cultured with BMP7 versus activin.

(F) Magnified images of glomerular podocytes generated from NPCs expanded with activin. COL4, type IV collagen. Arrowheads indicate pre-slit diaphragm domains; arrows indicate basal pre-slit diaphragm domains. Scale bar, 10 μm.

(G) H&E staining of kidney tissues generated from thawed NPCs at day 20 after spinal cord induction. Scale bar, 200 μm.

*(legend continued on next page)*

BMP7 concentration showed slightly better degrees of propagation and NPC marker retention.

Li et al. (2016) reported that the combination of BMP7, BMP receptor inhibitor LDN193189, and TGFβ receptor inhibitor A83-01 was effective for 7-month *in vitro* expansion of NPCs derived from human embryos. When we applied their conditions to our iPSC-derived ITGA8$^+$/PDGFRA$^-$/SIX2-GFP$^+$ cells, robust cell proliferation was observed and 71.5% of the cells remained SIX2-GFP$^+$ (Figures S2A and S2B). However, the percentages of the ITGA8$^+$/PDGFRA$^-$ fraction were low, even at day 7 of culture (25.5%), and only 18.2% of the expanded cells remained ITGA8$^+$/PDGFRA$^-$/SIX2-GFP$^+$. RT-PCR analysis showed that *SIX2* expression was relatively maintained, consistent with the high SIX2-GFP$^+$ cell percentage, but *Eya1* was reduced and a differentiation marker, *CDH1*, was increased at day 7 (Figure S2C). Therefore, monitoring of SIX2 expression alone could lead to over-estimation of the maintenance efficiency of NPCs.

## Activin Maintains NPCs at High Efficiency

Among the various reagents tested for improvement of the culture condition, such as BMP4, FGF10, FGF20, CXCL12, Wnt9b, and R-spondin, we found that TGFβ-related ligands, including activin, GDF11, TGFβ1, and TGFβ2, led to better maintenance of ITGA8$^+$/PDGFRA$^-$/SIX2-GFP$^+$ cells than BMP7 at day 7 of culture (Figure 3A). Among them, activin was the most effective: 91.6% of cells were SIX2-GFP$^+$ and up to 83.1% of cells remained ITGA8$^+$/PDGFRA$^-$/SIX2-GFP$^+$ (Figures 3A and S3). Furthermore, activin achieved 5.3 ± 0.8-fold expansion (n = 3) of NPCs, which was superior to BMP7 (Figure 3B). The expression levels of *SIX2* and other progenitor markers, as well as differentiation markers, were comparable with those at the starting point (day 0), in sharp contrast to those with BMP7 treatment (Figure 3C). Comprehensive RNA-seq and clustering analyses also placed the NPCs cultured with activin closer to those at the start of culture and in human embryos, compared with the NPCs cultured with BMP7 (Figure 4). The activin-based protocol maintained nephron progenitor markers, including *SIX2*, *SALL1*, *EYA1*, *CITED1*, *PAX2*, *WT1*, *MEOX1*, and *ITGA8*. Human NPC-specific genes, such as *LYPD1*, *TMEM100*, *WASF3*, *UNC5B*, and *PHF19*, which were recently identified in human embryos (Lindstrom et al., 2018b), were also maintained. In contrast, *SIX2* and *MEOX1* were significantly downregulated upon BMP7 treatment while differentiation markers (*LHX1*, *CDH1*, *HNF1B*, *JAG1*, *GATA3*, and *EMX2*) were upregulated. Therefore, activin can maintain human iPSC-derived ITGA8$^+$/PDGFRA$^-$/SIX2-GFP$^+$ NPCs more effectively than BMP7. Next, we examined the nephron-forming potential of the expanded cells. Cells expanded with activin or other TGFβ-related ligands exhibited robust formation of glomeruli and renal tubules at day 20 after spinal cord induction, and the areas of nephrogenesis were much larger than that for cells treated with BMP7 (Figures 3D and 3E, n = 6; Figure S4). Among them, activin showed the largest area of nephrogenesis (Figure S4, n = 3), and was thus selected for use in subsequent experiments. Notably, NEPHRIN$^+$ rod or dot-like structures were observed in the glomerular podocytes generated from activin-expanded NPCs. These structures were detected on the lateral domains of the podocytes, as well as on their basal domains adjacent to the type IV collagen (COL4)-positive basement membrane (Figure 3F). We recently reported that these structures observed in iPSC-derived kidney organoids represent the precursors of slit diaphragms, which play a critical role in filtration of blood to produce urine (Tanigawa et al., 2018). Thus, the activin-based protocol can retain NPCs at comparable quality to the start of the culture for the generation of these nephron structures.

We further examined whether the expanded NPCs could be frozen before induction to form nephrons. NPCs were cultured for 7 days with activin, frozen in single-cell suspensions, and thawed for regeneration of NPC spheres. When the spheres were induced with spinal cord they readily exhibited nephrogenesis, including glomerular podocytes with slit diaphragm precursors (Figures 3G–3I). The nephron areas constituted 79.8% ± 3.6% (n = 4), and were comparable with those of unfrozen progenitors. These results suggest that the complicated iPSC handling required for NPC induction can be bypassed by starting with frozen NPC stocks.

## Each of the Added Factors Is Required for Proper NPC Expansion

To confirm the requirement of each added factor for NPC maintenance and propagation, we excluded each factor from the optimized medium and performed assessment on day 7 of culture (Figure 5A). When activin was eliminated, the percentage of the ITGA8$^+$/PDGFRA$^-$/SIX2-GFP$^+$ fraction decreased dramatically to 42% as expected, while the non-progenitor cell numbers were increased

(H) Immunostaining of nephrons generated from thawed NPCs. CDH6 (green), NEPHRIN (red), and CDH1 (yellow) are shown. Scale bar, 200 μm.

(I) Magnified image of glomerular podocytes. Immunostaining for NEPHRIN (red) and COL4 (green) are shown. Arrowheads indicate pre-slit diaphragm domains; arrows indicate basal pre-slit diaphragm domains. Scale bar, 10 μm.

See also Figures S3 and S4.

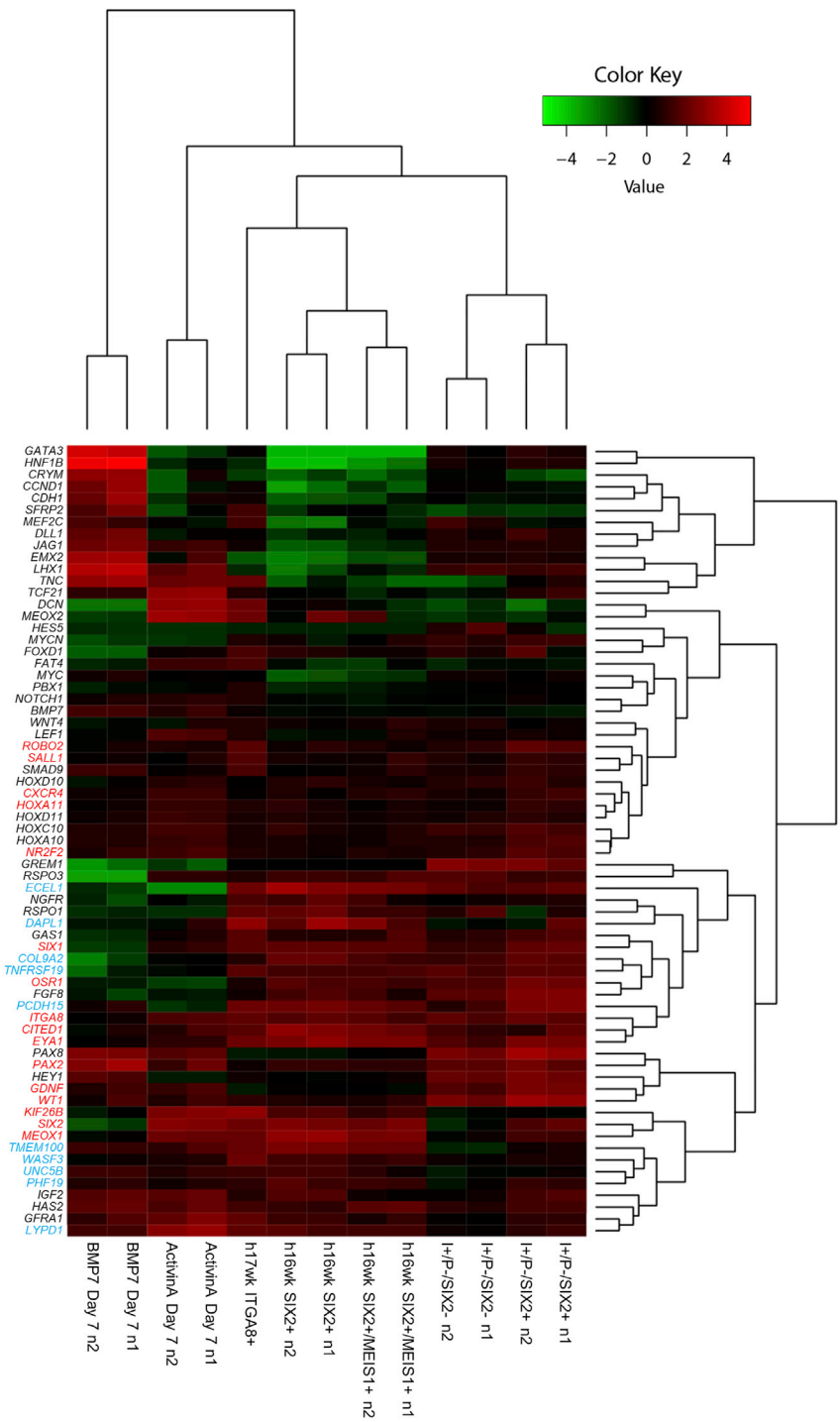


**Figure 4. RNA-Seq Analysis of the Propagated NPCs**

Heatmap and gene clustering of NPCs under the conditions listed below. Human NPCs from a 16- week embryonic kidney were used as a positive control (Lindstrom et al., 2018b). I+/P−/SIX2+, ITGA8$^+$/PDGFRA$^-$/SIX2-GFP$^+$ cells before expansion; I+/P−/SIX2−, ITGA8$^+$/PDGFRA$^-$/SIX2-GFP$^-$ cells before expansion; h16wk SIX2+/MEIS1+, hMARIS_SIX2$^+$_MEIS1$^+$ cells from a human 16-week embryonic kidney (Lindstrom et al., 2018b); h16wk SIX2+, hMARIS_SIX2$^+$ cells from a human 16-week embryonic kidney (Lindstrom et al., 2018b); h16wk ITGA8$^+$, ITGA8$^+$ cells from a human 17-week embryonic kidney (O'Brien et al., 2016); ActivinA Day 7, ITGA8$^+$/PDGFRA$^-$/SIX2-GFP$^+$ cells cultured with activin for 7 days; BMP7 Day 7, ITGA8$^+$/PDGFRA$^-$/SIX2-GFP$^+$ cells cultured with BMP7 for 7 days. NPC markers (Park et al., 2012) are shown in red. Human-specific NPC markers (Lindstrom et al., 2018b) are shown in blue.
See also Table S1.

(Figures 5A–5C). Depletion of DAPT significantly reduced the percentage of the progenitor fraction, as well as the numbers of progenitor cells. FGF9 elimination resulted in a sharp drop in the total cell numbers, indicating that this factor is essential for the proliferation of both progenitors and non-progenitors, consistent with our previous findings in mouse progenitor culture (Tanigawa et al., 2016). Elimination of LIF or CHIR did not affect the percentage of the progenitor fraction (Figures 5A and 5B), but the numbers of progenitor cells were significantly decreased (Figure 5C). Thus, each factor is necessary for proper NPC maintenance and propagation.

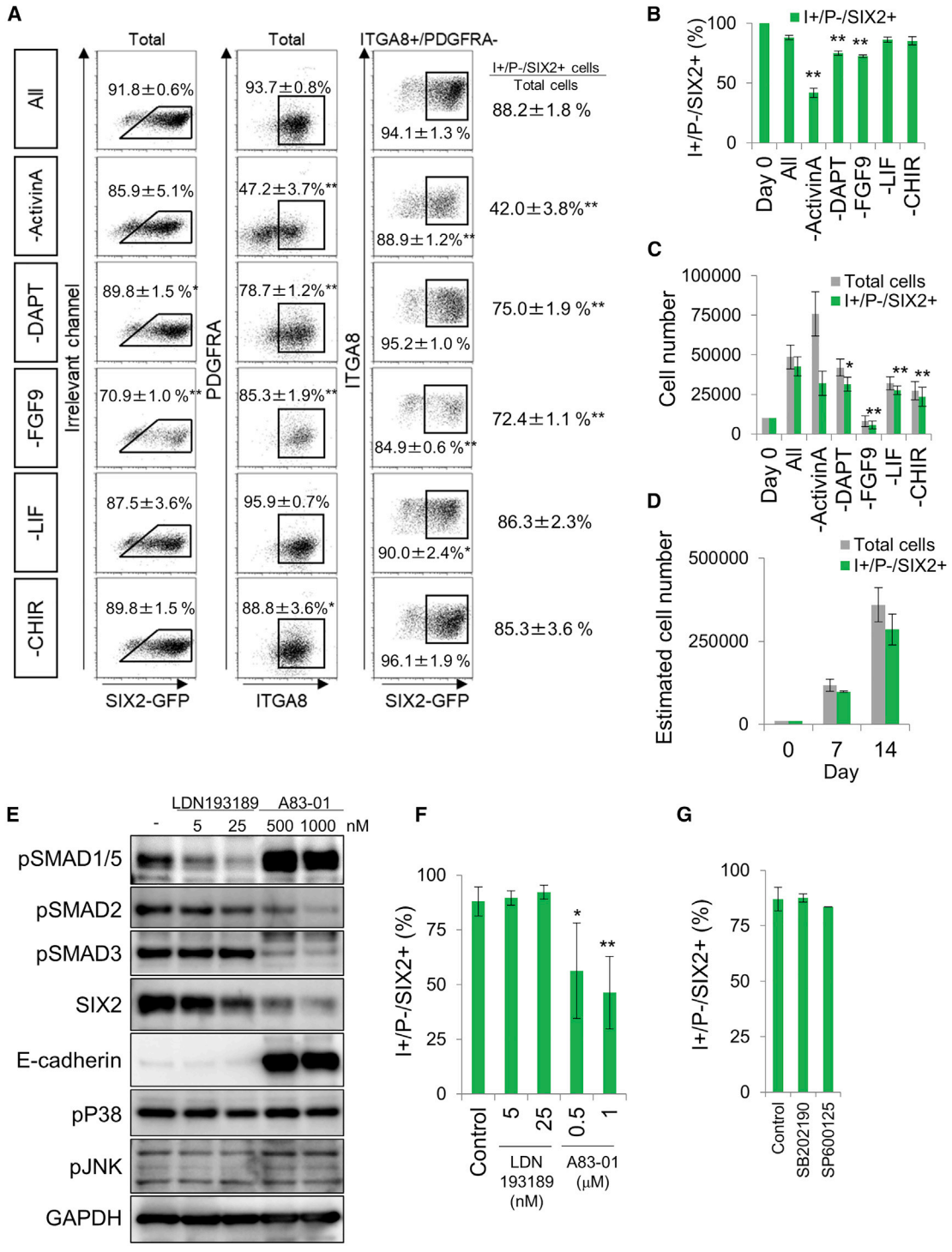


**Figure 5. Activin-Mediated Signal Is Essential for Maintenance of NPCs**

(A) Quantification of ITGA8$^+$/PDGFRA$^-$/SIX2-GFP$^+$ (I+/P−/SIX2+) cells after culture for 7 days. NPCs were cultured for 7 days in the optimized medium including activin (50 ng/mL) as indicated (All), and with individual factors eliminated from the optimized medium, then analyzed by flow cytometry. The percentages of ITGA8$^+$/PDGFRA$^-$/SIX2-GFP$^+$ cells in the total cells are shown on the right (I+/P−/SIX2+ cells/total cells) (n = 3 per group). *p < 0.05, **p < 0.01 versus All.

(B) Percentages of ITGA8$^+$/PDGFRA$^-$/SIX2-GFP$^+$ cells among the total cells (n = 3 per group). **p < 0.01 versus All.

*(legend continued on next page)*

When the expanded cells at day 7 were passaged and cultured for a further 7 days (day 14), NPCs increased by 25-fold and constituted 79.4% of the expanded cells (Figure 5D). Furthermore, progenitor cells retained comparable nephron-forming potential to day 7 (Figures S5A–S5C). However, the percentage of the ITGA8$^+$/PDGFRA$^-$/SIX2-GFP$^+$ fraction at day 21 (third generation of culture) declined to 57.3%, although the SIX2-GFP$^+$ fraction remained high (91.5%; Figure S5D), indicating that further fine-tuning or addition of an unknown signal is necessary for infinite maintenance of nephron progenitors. We also attempted monolayer cultures of single cells, but the percentage of the ITGA8$^+$/PDGFRA$^-$/SIX2-GFP$^+$ fraction at day 14 (second generation of culture) declined to 37.4% (Figures S5E and S5F), indicating that three-dimensional aggregation culture was better than two-dimensional culture.

## SMAD2/3 Phosphorylation Is Correlated with NPC Maintenance

To elucidate the mechanisms underlying the maintenance of NPCs, we examined the effects of BMP or TGFβ receptor inhibitors. When NPCs were cultured for 7 days using the activin-based protocol in the presence of BMP receptor inhibitor LDN193189 the phosphorylation levels of SMAD1/5 were reduced, while the percentage of the ITGA8$^+$/PDGFRA$^-$/SIX2-GFP$^+$ fraction was not affected (Figures 5E and 5F), indicating that BMP receptor-mediated SMAD1/5 activity had a minimal effect on NPC maintenance. In contrast, treatment with TGFβ receptor inhibitor A83-01 resulted in a reduction of SMAD2/3 phosphorylation and a decrease in the percentage of the ITGA8$^+$/PDGFRA$^-$/SIX2-GFP$^+$ fraction (Figures 5E and 5F). Consistent with the latter observation, SIX2 expression was reduced while E-cadherin was increased (Figure 5E). Unexpectedly, we observed increased SMAD1/5 phosphorylation upon A83-01 treatment (Figure 5E), which may reflect the higher percentage of differentiated cells in the samples, because SMAD1/5 activity is known to be detectable in differentiating nephrons (Brown et al., 2013; Fetting et al., 2014). Thus, phosphorylation of SMAD2/3, but not SMAD1/5, is correlated with NPC maintenance in our protocol.

It was reported that non-canonical BMP signaling molecules, namely JNK and p38, play critical roles in the maintenance and proliferation of NPCs (Brown et al., 2011; Muthukrishnan et al., 2015). However, the phosphorylation of p38 and JNK was unaltered by LDN193189 or A83-01 treatment (Figure 5E). In addition, p38 or JNK inhibitors had minimal impacts on the NPC percentages (Figure 5G), indicating that non-canonical BMP signaling is not significantly involved in our activin-based NPC maintenance. Thus, the canonical SMAD2/3 pathway downstream of activin may play a major role in the maintenance of human iPSC-derived NPCs.

## Propagated NPCs Form Large Areas of Nephrons with Vascularized Glomeruli upon Transplantation

Next, we examined the *in vivo* nephron-forming potential of the expanded NPCs. We cultured NPCs with activin for 7 days, combined the cells with spinal cord for a further 2 days to initiate nephrogenesis, and transplanted the spheres underneath the kidney capsule of immunodeficient mice, as previously described (Sharmin et al., 2016). In this setting, it is known that iPSC-derived NPCs can form glomeruli and renal tubules, the former of which are vascularized by host endothelial cells. Glomerular podocytes become more mature than those *in vitro*, and NEPHRIN is expressed at the basal side of the podocytes to form slit diaphragms, comprising molecular sieves for filtration from the vasculature (Tanigawa et al., 2018). As a control, we used whole spheres containing NPCs before maintenance culture, as described in our previous report (Sharmin et al., 2016). At day 20 after transplantation, the control cells showed formation of glomeruli and renal tubules (day 0 in Figure 6A). However, these nephrons constituted only a subset (10.3%, n = 3) of the transplanted tissues (Figures 6A and 6B). In contrast, nephrons derived from the expanded cells occupied larger areas of the transplanted tissues (70.1%, n = 3), suggesting good preservation of the NPC percentage and potential. In addition,

(C) Numbers of total and ITGA8$^+$/PDGFRA$^-$/SIX2-GFP$^+$ cells after culture for 7 days (n = 3 per group). *p < 0.05, **p < 0.01 versus All.
(D) Estimated numbers of total and ITGA8$^+$/PDGFRA$^-$/SIX2-GFP$^+$ cells after culture for 7 or 14 days. Data represent means ± SEM from three independent experiments.
(E) Western blotting analysis of cultured ITGA8$^+$/PDGFRA$^-$/SIX2-GFP$^+$ cells after treatment with BMP or TGFβ receptor inhibitors. NPCs were cultured in activin-containing medium with or without (−) inhibitors at the indicated concentrations for 7 days. The indicated molecules were detected by immunoblotting.
(F) Quantification of ITGA8$^+$/PDGFRA$^-$/SIX2-GFP$^+$ cells after culture for 7 days. NPCs were cultured for 7 days in activin-containing medium with or without (control) inhibitors at the indicated concentrations. The percentages of ITGA8$^+$/PDGFRA$^-$/SIX2-GFP$^+$ cells were measured by flow cytometry. Data represent means ± SEM from three independent experiments. *p < 0.05, **p < 0.01 versus control.
(G) NPCs were cultured for 7 days in activin-containing medium with p38 inhibitor SB202190 (1 μM) or JNK inhibitor SP600125 (1 μM). The percentages of ITGA8$^+$/PDGFRA$^-$/SIX2-GFP$^+$ cells were measured by flow cytometry (n = 3 per group).
See also Figure S5.

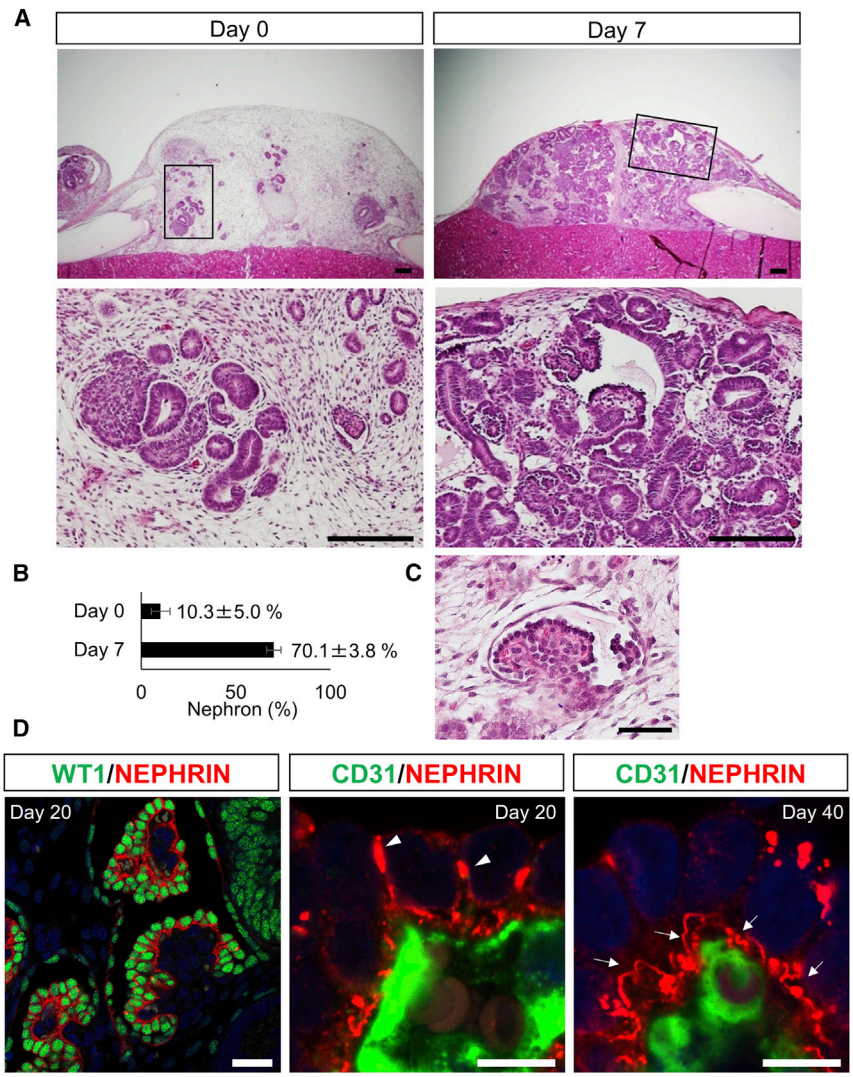


**Figure 6. Propagated NPCs Form Large Areas of Nephrons with Vascularized Glomeruli upon Transplantation**

(A) H&E-stained sections of tissues at 20 days after transplantation. Left panels: transplants from iPSC-derived NPCs before expansion culture (without sorting). Right panels: transplants from ITGA8$^+$/PDGFRA$^-$/SIX2-GFP$^+$ cells cultured with activin for 7 days. Scale bars, 50 μm. The bottom panels show magnified images of the squares in the upper panels. Scale bars, 200 μm.

(B) Quantification of nephron areas in induced tissues. The percentages of nephron structures in the induced tissues relative to the total section areas were calculated and shown as bar graphs (n = 3 per group).

(C) Magnified image of a glomerulus in transplants of ITGA8$^+$/PDGFRA$^-$/SIX2-GFP$^+$ cells. Scale bar, 50 μm.

(D) Immunostaining of glomeruli. Transplants of ITGA8$^+$/PDGFRA$^-$/SIX2-GFP$^+$ cells after 20 and 40 days were stained for NEPHRIN (red) and WT1 (green) or CD31 (green). The immunostained images show vascularized glomeruli and basolateral localization of NEPHRIN at 20 days (left and center) and 40 days (right) after transplantation. Arrowheads indicate lateral pre-slit diaphragm domains; arrows indicate basal linear expression of NEPHRIN. Scale bars, 25 μm (left); and 8 μm (center and right).

NEPHRIN was expressed in glomerular podocytes at their basal side and aligned in a linear manner along the endothelial cells (Figures 6C and 6D), which is characteristic of maturation-stage podocytes equipped with basally located slit diaphragms (Tanigawa et al., 2018). These data indicate that the ITGA8$^+$/PDGFRA$^-$/SIX2-GFP$^+$ NPCs propagated by activin retain their nephron-forming competence *in vivo* and can successfully generate maturation-stage glomerular podocytes, further supporting the authenticity of our protocol.

## The Activin-Based Protocol Is Applicable to iPSC Lines without a GFP Tag

Next, we examined whether our protocol was applicable to multiple iPSC lines. We further investigated the expansion of NPCs from iPSCs without a GFP tag, which would make our protocol more useful. For this, we established two new iPSC lines (RN7 and RN12) from a healthy donor using a Sendai virus vector. Both iPSC lines had normal karyotypes and expressed pluripotent stem cell markers (Figures 7A, 7B, and S6).

First, we induced the RN7 line toward the kidney lineage, sorted the ITGA8$^+$/PDGFRA$^-$ cells at day 13, and cultured them for 7 days with activin or BMP7. In the presence of activin, cells were expanded by 11-fold and 90% of the cells were ITGA8$^+$/PDGFRA$^-$ (Figure 7C). In contrast, only a 4.4-fold increase was observed in the presence of BMP7, although 84% of the expanded cells were ITGA8$^+$/PDGFRA$^-$ (Figure 7C). Intriguingly, staining of cytospun cells from the ITGA8$^+$/PDGFRA$^-$ fraction revealed that 85.1% of cells were SIX2$^+$ in the presence of activin, compared with only 3.4% of SIX2$^+$ cells in the presence of BMP7 (Figure 7D). The expression level of *SIX2* was significantly reduced in the BMP7 condition (Figure 7E). When the cells expanded by activin were induced for differentiation, they readily formed glomeruli and renal

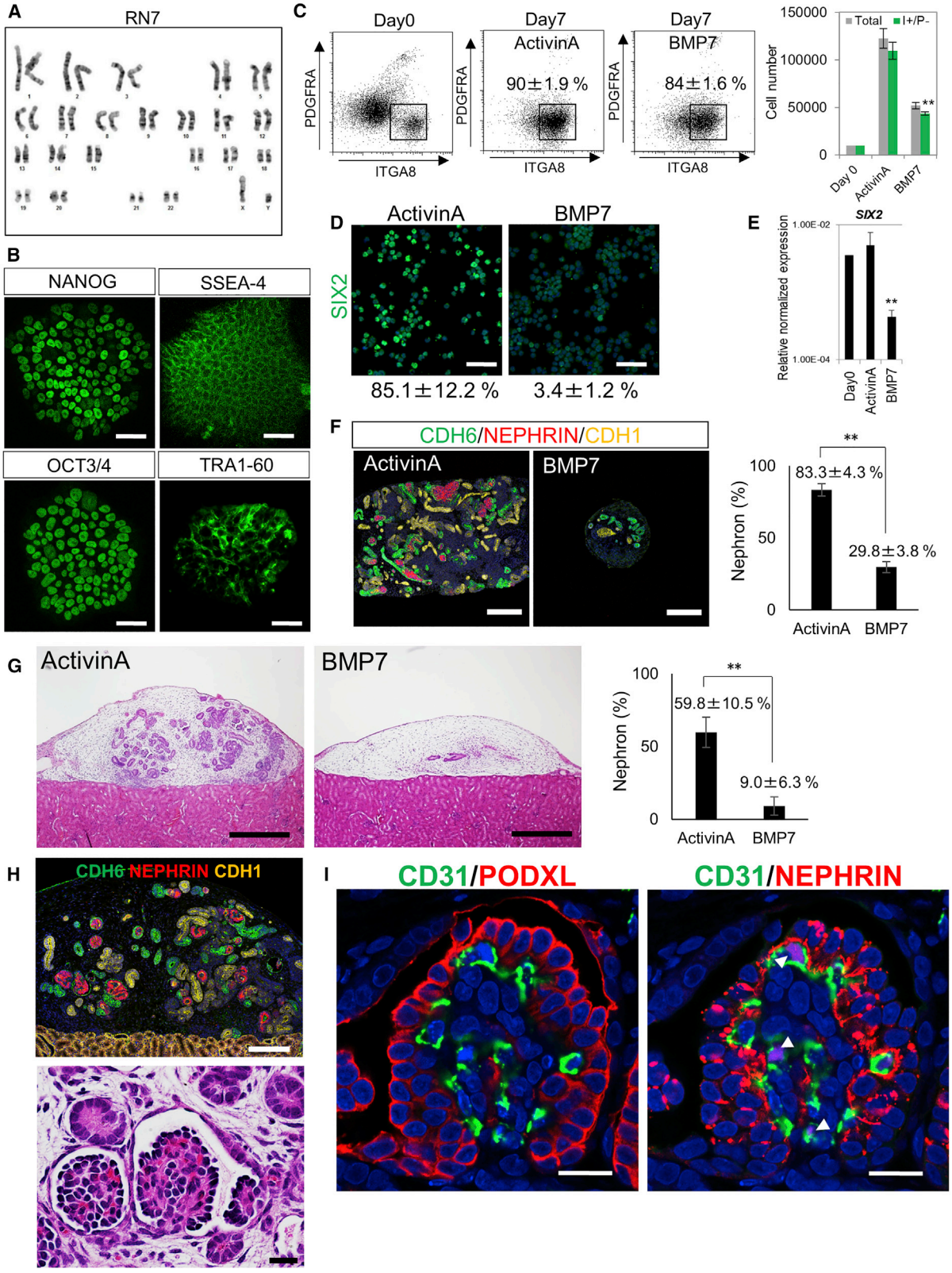


*(legend on next page)*

tubules, and the percentages of the nephron area were larger than those of cells cultured with BMP7 (Figure 7F, n = 6). Finally, the expanded cells were transplanted under the renal capsules of immunodeficient mice as described above. At day 20 after transplantation, the cells expanded by activin showed robust formation of glomeruli and renal tubules (Figures 7G and 7H, n = 4). The percentages of the nephron area in the transplanted tissues were larger than those of cells cultured with BMP7 (Figure 7G, n = 4). Round and vascularized glomeruli were formed that resembled those in transplanted human embryonic kidneys (Dekel et al., 2003). The glomeruli contained podocytes positive for PODOCALYXIN (PODXL), and NEPHRIN was linearly aligned with CD31$^+$ vascular endothelial cells (Figure 7I). In contrast, cells expanded by BMP7 showed minimal formation of nephrons upon transplantation (Figure 7G). All of these tendencies held true for the RN12 cell line (Figure S6). Thus, activin exhibits superior effects to BMP7 for NPC expansion and nephrogenesis *in vitro* and *in vivo*, and our protocol is applicable to multiple independent iPSC lines as well as genetically untagged clones.

## DISCUSSION

We have demonstrated that activin exerts a superior effect to BMP7 on the maintenance of NPCs derived from human iPSCs. The percentage of ITGA8$^+$/PDGFRA$^-$/SIX2-GFP$^+$ progenitors remained high in our activin-based protocol, and the resulting nephrons occupied the majority of the induced tissues both *in vitro* and *in vivo*. Our improved protocol depends on quantitative measurement of nephron progenitors based on three markers. While monitoring of SIX2 expression with GFP is useful, we demonstrated that dependence on SIX2 expression alone is insufficient and further combination with two other markers (ITGA8$^+$/PDGFRA$^-$) is essential for assessment of nephron-forming competence.

Based on these stringent criteria, we identified that activin is superior to BMP7 in maintaining human iPSC-derived NPCs. We and others previously reported the importance of BMP7 for NPC propagation in both mice and humans. Li et al. (2016) claimed that human iPSC-derived SIX2-GFP$^+$ cells are expandable for 2 months. However, when we applied the same protocol, the percentage of ITGA8$^+$/PDGFRA$^-$/SIX2-GFP$^+$ cells was low, while that of SIX2-GFP$^+$ cells remained relatively high, again emphasizing the importance of the progenitor criteria. In contrast, our activin-based protocol maintained 80%–90% of the expanded cells as ITGA8$^+$/PDGFRA$^-$/SIX2-GFP$^+$. Upon transplantation, nephron epithelia derived from the expanded progenitors occupied large areas of the induced tissues and glomerular podocytes exhibited the characteristic features of those *in vivo*: NEPHRIN was localized at the basal region of the podocytes and aligned with the podocyte-endothelial boundary, underscoring the high percentage and quality of our expanded nephron progenitors. In addition, we demonstrated that the expanded cells could be frozen without losing their nephron-forming potential, suggesting that the complicated induction processes for NPCs can be bypassed for certain sets of experiments. Furthermore, our

**Figure 7. The Activin-Based Protocol Is Applicable to iPSC Lines without a GFP Tag**

(A) Normal karyotype of an established iPSC clone (RN7) from a healthy donor.

(B) Expression of stem cell markers in RN7 iPSCs. Scale bars, 200 μm.

(C) Flow-cytometry analysis of the ITGA8$^+$/PDGFRA$^-$ fraction after a 7- day expansion culture of NPCs induced from RN7. Day 0: ITGA8$^+$/PDGFRA$^-$ fraction of induced NPCs before expansion culture. The percentages of the ITGA8$^+$/PDGFRA$^-$ fraction after 7 days of culture with activin or BMP7 are shown (n = 3 per group). Rightmost panel: numbers of total and ITGA8$^+$/PDGFRA$^-$ (I+/P−) cells after 7 days of culture (n = 3 per group). **p < 0.01, cells cultured with activin versus BMP7.

(D) SIX2 staining of cytospun ITGA8$^+$/PDGFRA$^-$ cells at day 7 of expansion culture. The percentages of SIX2$^+$ cells among the ITGA8$^+$/PDGFRA$^-$ cells are also shown (n = 3 per group).

(E) qPCR analysis of *SIX2* expression in ITGA8$^+$/PDGFRA$^-$ cells after culture for 7 days. Freshly isolated ITGA8$^+$/PDGFRA$^-$ cells were used as a positive control (Day 0). **p < 0.01, cells cultured with activin or BMP7 versus Day 0 (n = 3 per group).

(F) Immunostaining of nephron structures generated from RN7-derived ITGA8$^+$/PDGFRA$^-$ cells expanded by activin or BMP7 for 7 days. Scale bars: 200 μm. Right panel: percentages of nephron-like structures in the induced tissues are shown as bar graphs. Data represent means ± SEM from three independent experiments. **p < 0.01, cells cultured with activin versus BMP7.

(G) H&E-stained sections of kidney tissues at 20 days after transplantation. Left panels: transplants from RN7-derived ITGA8$^+$/PDGFRA$^-$ cells cultured with activin (left) or BMP7 (right) for 7 days. Scale bars, 100 μm. Rightmost panel: percentages of nephron areas in transplanted tissues (n = 4 per group). **p < 0.01, cells cultured with activin versus BMP7.

(H) Immunostaining of nephron structures (upper panel) and H&E-staining of a glomerulus (lower panel) in the transplants from RN7-derived ITGA8$^+$/PDGFRA$^-$ cells cultured with activin. Scale bars, 200 μm (upper panel) and 50 μm (lower panel).

(I) Immunostaining of glomeruli in kidney tissues at 20 days after transplantation of RN7-derived NPCs. CD31 (green) and PODXL (red) or NEPHRIN (red) are shown. Arrowheads indicate background signals of red blood cells. Scale bars, 25 μm.

See also Figure S6.

activin-based protocol was applicable to multiple iPSC lines, proving its robustness.

It was an unexpected finding that activin is superior to BMP7 for NPC maintenance. Most published maintenance protocols are based on the importance of BMP7, especially the non-canonical pathway downstream of BMP7, while SMAD1 induces NPC differentiation. For example, Li et al. (2016) reported maintenance of NPCs from human embryos utilizing BMP7 and a BMP receptor inhibitor, resulting in SMAD1 inhibition. Meanwhile, expression of activin receptor type II or phosphorylated Smad2 in the nephron progenitor regions was reported in mice (Rowan et al., 2018). Furthermore, deletion of *GDF11*, which is expressed in nephron progenitors and the ureteric bud, led to kidney hypoplasia (Esquela and Lee, 2003). These reports may be relevant to our present finding that the activin/GDF11/TGFβ-SMAD2/3 pathway is involved in NPC maintenance *in vitro*. Alternatively, the responsiveness to exogenous signals may differ between *in vivo* NPCs and iPSC-derived NPCs. While further investigation is required to address these possibilities, our data emphasize the practical usefulness of the activin-based protocol, considering the limited access to human embryos.

However, our protocol did not achieve long-term propagation. Consistent with this limitation, our RNA-seq analysis showed incomplete preservation of the gene expression profiles during culture (Figure 4). For example, *SIX1* and *OSR1* were decreased, which may explain the limited propagation and longevity of the nephron progenitors under our conditions. Among the human nephron progenitor-specific genes that were recently identified in human embryos, *ECEL1*, *DAPL1*, *COL9A2*, *TNFRSF19*, and *PCDH15* were reduced (Figure 4). To improve our protocol, information on the expression levels of these genes in human embryonic NPCs at the equivalent stage to iPSC-derived NPCs is needed for reference. RNA-seq data at 16 weeks of gestation (Lindstrom et al., 2018b), which were used for comparison in this study, are helpful, but gene expression levels in nephron progenitors change significantly over time *in vivo* (Chen et al., 2015). Data at an earlier time point (4–5 weeks after fertilization), when human nephron progenitors initially emerge, would be needed for precise comparisons. Nonetheless, our data provide the essential gene set that can confer sufficient competence to human nephron progenitors.

Although our protocol is applicable to multiple iPSC lines without a GFP tag, identification of additional surface markers would improve the maintenance efficiency of NPCs. It was reported that NPCs could be enriched in NCAM$^+$/CD133$^-$/FZD7$^+$ or NCAM$^+$/CD133$^-$/EpCAM$^-$ fractions from human fetal kidneys at 15–22 weeks (Harari-Steinberg et al., 2013; Pode-Shakked et al., 2016, 2017), and that some NPC genes were maintained during 2 weeks of culture. The NGFR$^+$/EPCAM$^-$ fraction was also used for NPC isolation from human embryonic kidneys at 9–14 weeks (Li et al., 2016). However, our RNA-seq analysis showed that the expression of *NCAM*, *FZD7*, and *NGFR* were relatively lower than that of *ITGA8* in iPSC-derived NPCs (ITGA8$^+$/PDGFRA$^-$/SIX2-GFP$^+$) before expansion, while the same genes were expressed to some extent in SIX2$^+$ NPCs in human embryonic kidneys at 16 weeks (Table S1). Indeed, Li et al. (2016) reported that NGFR was not applicable to iPSC-derived NPCs, and our preliminary trials on these three markers for isolation of iPSC-derived NPCs were also unsuccessful. These results may indicate that artificially induced NPCs are not completely identical to those *in vivo*. Alternatively, iPSC-derived NPCs could represent those at 4–5 weeks of gestation when NPCs first appear *in vivo* (Lindstrom et al., 2018a). Establishment of the gene expression profiles in human embryonic NPCs at earlier time points will be helpful toward the identification of more reliable surface markers for iPSC-derived NPCs.

Nonetheless, our protocol will be useful for a variety of settings in iPSC-based research. Differentiation efficiencies vary from clone to clone, and can sometimes be very low. Even in these situations, our protocol allows propagation of NPCs with high efficiency, and the cells can be subjected to subsequent functional assays for nephrogenesis *in vitro* and *in vivo*. We recently reported that iPSCs derived from a patient with a NEPHRIN mutation showed impaired formation of slit diaphragms in podocytes (Tanigawa et al., 2018). We also established a selective podocyte induction protocol from human iPSCs (Yoshimura et al., 2019). Combined with these two methods, our expansion protocol would be readily applicable for disease modeling and drug screening using patient-derived iPSCs. We also reported the generation of branching ureteric buds from mouse ESCs and human iPSCs *in vitro* (Taguchi and Nishinakamura, 2017). When mouse ESC-derived nephron progenitors and ureteric bud were combined with mouse embryo-derived stromal cells, we were able to reconstitute a higher-order kidney structure *in vitro*. While we need to induce stromal progenitors from human iPSCs, our method for expansion of nephron progenitors will be useful for reconstructing a three-dimensional human kidney in the near future.

In summary, we have developed an activin-based protocol for maintenance and propagation of iPSC-derived human NPCs at high efficiency, which can serve as a solid basis for regenerative medicine of the kidney.

## EXPERIMENTAL PROCEDURES

### Establishment of *SIX2-GFP* iPSCs

We established *SIX2-GFP* iPSCs by transfecting the targeting vector, along with the TALEN expression plasmids (Sakuma et al., 2013), into human iPSCs (201B7) (Takahashi et al., 2007). A full

description of the methods is provided in Supplemental Experimental Procedures. We obtained 23 heterozygous GFP-knockin clones among 91 clones, as determined by PCR, Southern blotting, and sequencing of the non-GFP-containing allele. Clone #12 was adapted to the feeder-free condition using StemFit AK02N medium (Takara Bio, AJ100) and plates coated with iMatrix-511 silk (Nippi, #892021), as described previously (Nakagawa et al., 2014; Yoshimura et al., 2017), and further electroporated with a plasmid expressing Cre recombinase to delete the puromycin-resistant cassette. The resultant colonies were picked up in duplicate and puromycin-sensitive clones were expanded. The absence of the cassette was verified by PCR, and clones #12-8 and #12-12 were used for detailed analyses. We used clone #12-12 for most of the presented data, but consistent data were obtained for clone #12-8 (see Figure S3).

### Propagation of Human iPSC-Derived NPCs

NPC induction was performed based on our previously established protocol (Taguchi et al., 2014; Taguchi and Nishinakamura, 2017). Induced NPCs were dissociated by incubation with AccuMAX (Millipore) for 8 min, and IGTA8$^+$/PGDFRA$^-$/SIX2-GFP$^+$ NPCs were sorted as described by Kaku et al. (2017). The sorted NPCs were aggregated as described by Tanigawa et al. (2016) in the following maintenance medium. The maintenance medium for NPCs comprised 200 ng/mL recombinant human FGF9 ( R&D Systems), 10 ng/mL recombinant human TGFα (Peprotech), 1 μg/mL heparin (Sigma), 10 μM Y27632 (Wako Chemicals), 500 nM CHIR99021 (Axon Medchem), 5 ng/mL recombinant human LIF (Millipore), 500 nM DAPT (Millipore), and 50 ng/mL recombinant human activin A (R&D Systems) in the medium used for NPC induction from iPSCs (Taguchi et al., 2014). The chemical compounds investigated for NPC culture were as follows: A83-01 (Tocris, #2939); LDN193189 (Wako, #126-05851); SB202190 (Sigma, #S7067); and SP600125 (Wako, #198-14821). For passaging, the cells were rinsed with PBS, dissociated with AccuMAX for 8 min, and split at a 1:3 ratio for passage every 7 days. For cryopreservation, 7- day cultured cells were rinsed with PBS and dissociated with AccuMAX for 8 min. After centrifugation, the cells were washed with medium containing 50 ng/mL DNase I, resuspended (100,000 cells/vial) in Stem Cell Banker (Nippon Zenyaku Kogyo), and stored in liquid nitrogen after 24 h of pre-storage at −80°C. Defrosted cells were incubated overnight in maintenance medium to allow aggregate formation on low-binding 96-well plates (Tanigawa et al., 2016). NPC aggregates were cultured with embryonic spinal cord for 3 days to initiate differentiation, transferred to transwell plates, and cultured for an additional 9–20 days in previously described medium (Li et al., 2016) containing 5% KnockOut Serum Replacement (Thermo Fisher Scientific).

### Establishment of New iPSC Lines

Two iPSC lines (RN7 and RN12) were established from the peripheral blood of a healthy volunteer using a previously described method (Soga et al., 2015). In brief, four reprogramming transcription factors (OCT3/4, SOX2, KLF4, and MYC) were introduced using a Sendai virus vector. After establishing the iPSC clones on feeder cells (murine embryonic fibroblasts), the temperature-sensitive Sendai virus was eliminated by culturing the cells at 38°C for 24 h. Elimination of the exogenous genes was confirmed by nested PCR of the vector sequences. RN7 and RN12 cells were adapted to the feeder-free condition using StemFit AK02N medium and plates coated with iMatrix-511 silk, as described previously (Nakagawa et al., 2014; Yoshimura et al., 2017). NPC induction was performed based on our previously established protocol (Taguchi et al., 2014; Taguchi and Nishinakamura, 2017).

All animal experiments were carried out in accordance with our institutional guidelines and were approved by the Ethics Committee of Kumamoto University (#A29-040). The ethics committees involved were the Ethics Committee for Epidemiological and General Research at the Faculty of Life Science, Kumamoto University, and the Ethics Committee for Human Genome and Gene Analysis Research at the Faculty of Life Science, Kumamoto University (approval numbers 1453 and 359, respectively).

### Statistical Analysis

All experiments were performed independently at least three times. Data are presented as mean ± SEM. Data were evaluated by Student's t test. Differences were considered significant for values of $p < 0.01$.

## ACCESSION NUMBERS

The accession number for the RNA-seq data deposited with the National Center for Biotechnology Information Gene Expression Omnibus is GEO: GSE118729.

## SUPPLEMENTAL INFORMATION

Supplemental Information can be found online at https://doi.org/10.1016/j.stemcr.2019.07.003.

## AUTHOR CONTRIBUTIONS

Culture and analysis of iPSC-derived NPCs, S.T.; generation of SIX2-GFP iPSCs, Y.K.; transplantation, H.N.; TALEN construction, T.S. and T.Y.; providing NPC induction protocol, A.T.; writing, S.T., A.T., and R.N.; Funding acquisition, S.T. and R.N.; Project administration, R.N.

## ACKNOWLEDGMENTS

We thank Tomoko Ohmori, Yumi Soejima, Koichiro Miike, and Sayoko Fujimura for technical assistance, and Drs. Masaki Hosoya and Yoshiharu Sato for the RNA-seq analysis. We also thank Alison Sherwin, PhD, from Edanz Group (www.edanzediting.com/ac) for editing a draft of the manuscript. This study was supported, in part, by KAKENHI grants (JP16K19494 to S.T. and JP17H06177 to R.N.) from the Japan Society for the Promotion of Science, and a grant from the Research Center Network for Realization of Regenerative Medicine, Japan Agency for Medical Research and Development. This work was also supported, in part, by The Mochida Memorial Foundation for Medical and Pharmaceutical Research.

Received: August 17, 2018
Revised: July 1, 2019
Accepted: July 1, 2019
Published: August 1, 2019

## REFERENCES


Barak, H., Huh, S.H., Chen, S., Jeanpierre, C., Martinovic, J., Parisot, M., Bole-Feysot, C., Nitschke, P., Salomon, R., Antignac, C., et al. (2012). FGF9 and FGF20 maintain the stemness of nephron progenitors in mice and man. Dev. Cell *22*, 1191–1207.

Brown, A.C., Adams, D., de Caestecker, M., Yang, X., Friesel, R., and Oxburgh, L. (2011). FGF/EGF signaling regulates the renewal of early nephron progenitors during embryonic development. Development *138*, 5099–5112.

Brown, A.C., Muthukrishnan, S.D., Guay, J.A., Adams, D.C., Schafer, D.A., Fetting, J.L., and Oxburgh, L. (2013). Role for compartmentalization in nephron progenitor differentiation. Proc. Natl. Acad. Sci. U S A *110*, 4640–4645.

Brown, A.C., Muthukrishnan, S.D., and Oxburgh, L. (2015). A synthetic niche for nephron progenitor cells. Dev. Cell *34*, 229–241.

Chen, S., Brunskill, E.W., Potter, S.S., Dexheimer, P.J., Salomonis, N., Aronow, B.J., Hong, C.I., Zhang, T., and Kopan, R. (2015). Intrinsic age-dependent changes and cell-cell contacts regulate nephron progenitor lifespan. Dev. Cell *35*, 49–62.

Costantini, F., and Kopan, R. (2010). Patterning a complex organ: branching morphogenesis and nephron segmentation in kidney development. Dev. Cell *18*, 698–712.

Dekel, B., Burakova, T., Arditti, F.D., Reich-Zeliger, S., Milstein, O., Aviel-Ronen, S., Rechavi, G., Friedman, N., Kaminski, N., Passwell, J.H., et al. (2003). Human and porcine early kidney precursors as a new source for transplantation. Nat. Med. *9*, 53–60.

Esquela, A.F., and Lee, S.J. (2003). Regulation of metanephric kidney development by growth/differentiation factor 11. Dev. Biol. *257*, 356–370.

Fetting, J.L., Guay, J.A., Karolak, M.J., Iozzo, R.V., Adams, D.C., Maridas, D.E., Brown, A.C., and Oxburgh, L. (2014). FOXD1 promotes nephron progenitor differentiation by repressing decorin in the embryonic kidney. Development *141*, 17–27.

Harari-Steinberg, O., Metsuyanim, S., Omer, D., Gnatek, Y., Gershon, R., Pri-Chen, S., Ozdemir, D.D., Lerenthal, Y., Noiman, T., Ben-Hur, H., et al. (2013). Identification of human nephron progenitors capable of generation of kidney structures and functional repair of chronic renal disease. EMBO Mol. Med. *5*, 1556–1568.

Hartman, H.A., Lai, H.L., and Patterson, L.T. (2007). Cessation of renal morphogenesis in mice. Dev. Biol. *310*, 379–387.

Kaku, Y., Taguchi, A., Tanigawa, S., Haque, F., Sakuma, T., Yamamoto, T., and Nishinakamura, R. (2017). PAX2 is dispensable for in vitro nephron formation from human induced pluripotent stem cells. Sci. Rep. *7*, 4554.

Kobayashi, A., Valerius, M.T., Mugford, J.W., Carroll, T.J., Self, M., Oliver, G., and McMahon, A.P. (2008). Six2 defines and regulates a multipotent self-renewing nephron progenitor population throughout mammalian kidney development. Cell Stem Cell *3*, 169–181.

Li, Z., Araoka, T., Wu, J., Liao, H.K., Li, M., Lazo, M., Zhou, B., Sui, Y., Wu, M.Z., Tamura, I., et al. (2016). 3D culture supports long-term expansion of mouse and human nephrogenic progenitors. Cell Stem Cell *19*, 516–529.

Lindstrom, N.O., McMahon, J.A., Guo, J., Tran, T., Guo, Q., Rutledge, E., Parvez, R.K., Saribekyan, G., Schuler, R.E., Liao, C., et al. (2018a). Conserved and divergent features of human and mouse kidney organogenesis. J. Am. Soc. Nephrol. *29*, 785–805.

Lindstrom, N.O., Guo, J., Kim, A.D., Tran, T., Guo, Q., De Sena Brandine, G., Ransick, A., Parvez, R.K., Thornton, M.E., Basking, L., et al. (2018b). Conserved and divergent features of mesenchymal progenitor cell types within the cortical nephrogenic niche of the human and mouse kidney. J. Am. Soc. Nephrol. *29*, 806–824.

Morizane, R., Lam, A.Q., Freedman, B.S., Kishi, S., Valerius, M.T., and Bonventre, J.V. (2015). Nephron organoids derived from human pluripotent stem cells model kidney development and injury. Nat. Biotechnol. *33*, 1193–1200.

Muller, U., Wang, D., Denda, S., Meneses, J.J., Pedersen, R.A., and Reichardt, L.F. (1997). Integrin alpha8beta1 is critically important for epithelial-mesenchymal interactions during kidney morphogenesis. Cell *88*, 603–613.

Muthukrishnan, S.D., Yang, X., Friesel, R., and Oxburgh, L. (2015). Concurrent BMP7 and FGF9 signalling governs AP-1 function to promote self-renewal of nephron progenitor cells. Nat. Commun. *6*, 10027.

Nakagawa, M., Taniguchi, Y., Senda, S., Takizawa, N., Ichisaka, T., Asano, K., Morizane, A., Doi, D., Takahashi, J., Nishizawa, M., et al. (2014). A novel efficient feeder-free culture system for the derivation of human induced pluripotent stem cells. Sci. Rep. *4*, 3594.

O'Brien, L.L., Guo, Q., Lee, Y., Tran, T., Benazet, J.D., Whitney, P.H., Valouev, A., and McMahon, A.P. (2016). Differential regulation of mouse and human nephron progenitors by the Six family of transcriptional regulators. Development *143*, 595–608.

Park, J.S., Ma, W., O'Brien, L.L., Chung, E., Guo, J.J., Cheng, J.G., Valerius, M.T., McMahon, J.A., Wong, W.H., and McMahon, A.P. (2012). Six2 and Wnt regulate self-renewal and commitment of nephron progenitors through shared gene regulatory networks. Dev. Cell *23*, 637–651.

Pode-Shakked, N., Gershon, R., Tam, G., Omer, D., Gnatek, Y., Kanter, I., Oriel, S., Katz, G., Harari-Steinberg, O., Kalisky, T., et al. (2017). Evidence of in vitro preservation of human nephrogenesis at the single-cell level. Stem Cell Reports *9*, 279–291.

Pode-Shakked, N., Pleniceanu, O., Gershon, R., Shukrun, R., Kanter, I., Bucris, E., Pode-Shakked, B., Tam, G., Tam, H., Caspi, R., et al. (2016). Dissecting stages of human kidney development and tumorigenesis with surface markers affords simple prospective purification of nephron stem cells. Sci. Rep. *6*, 23562.

Rowan, C.J., Li, W., Martirosyan, H., Erwood, S., Hu, D., Kim, Y.K., Sheybani-Deloui, S., Mulder, J., Blake, J., Chen, L., et al. (2018). Hedgehog-GLI signaling in Foxd1-positive stromal cells promotes murine nephrogenesis via TGFbeta signaling. Development *145*. https://doi.org/10.1242/dev.159947.

Sakuma, T., Ochiai, H., Kaneko, T., Mashimo, T., Tokumasu, D., Sakane, Y., Suzuki, K., Miyamoto, T., Sakamoto, N., Matsuura, S., et al. (2013). Repeating pattern of non-RVD variations in DNA-binding modules enhances TALEN activity. Sci. Rep. *3*, 3379.

Sharmin, S., Taguchi, A., Kaku, Y., Yoshimura, Y., Ohmori, T., Sakuma, T., Mukoyama, M., Yamamoto, T., Kurihara, H., and Nishinakamura, R. (2016). Human induced pluripotent stem cell-derived podocytes mature into vascularized glomeruli upon experimental transplantation. J. Am. Soc. Nephrol. *27*, 1778–1791.

Soga, M., Ishitsuka, Y., Hamasaki, M., Yoneda, K., Furuya, H., Matsuo, M., Ihn, H., Fusaki, N., Nakamura, K., Nakagata, N., et al. (2015). HPGCD outperforms HPBCD as a potential treatment for Niemann-Pick disease type C during disease modeling with iPS cells. Stem Cells *33*, 1075–1088.

Takahashi, K., Tanabe, K., Ohnuki, M., Narita, M., Ichisaka, T., Tomoda, K., and Yamanaka, S. (2007). Induction of pluripotent stem cells from adult human fibroblasts by defined factors. Cell *131*, 861–872.

Taguchi, A., Kaku, Y., Ohmori, T., Sharmin, S., Ogawa, M., Sasaki, H., and Nishinakamura, R. (2014). Redefining the in vivo origin of metanephric nephron progenitors enables generation of complex kidney structures from pluripotent stem cells. Cell Stem Cell *14*, 53–67.

Taguchi, A., and Nishinakamura, R. (2017). Higher-order kidney organogenesis from pluripotent stem cells. Cell Stem Cell *21*, 730–746.

Takasato, M., Er, P.X., Chiu, H.S., Maier, B., Baillie, G.J., Ferguson, C., Parton, R.G., Wolvetang, E.J., Roost, M.S., Lopes, S.M., et al. (2016). Kidney organoids from human iPS cells contain multiple lineages and model human nephrogenesis. Nature *536*, 238.

Tanigawa, S., Islam, M., Sharmin, S., Naganuma, H., Yoshimura, Y., Haque, F., Era, T., Nakazato, H., Nakanishi, K., Sakuma, T., et al. (2018). Organoids from nephrotic disease-derived iPSCs identify impaired NEPHRIN localization and slit diaphragm formation in kidney podocytes. Stem Cell Reports *11*, 727–740.

Tanigawa, S., Sharma, N., Hall, M.D., Nishinakamura, R., and Perantoni, A.O. (2015). Preferential propagation of competent SIX2$^{+}$ nephronic progenitors by LIF/ROCKi treatment of the metanephric mesenchyme. Stem Cell Reports *5*, 435–447.

Tanigawa, S., Taguchi, A., Sharma, N., Perantoni, A.O., and Nishinakamura, R. (2016). Selective in vitro propagation of nephron progenitors derived from embryos and pluripotent stem cells. Cell Rep. *15*, 801–813.

Yoshimura, Y., Taguchi, A., and Nishinakamura, R. (2017). Generation of a three-dimensional kidney structure from pluripotent stem cells. Methods Mol. Biol. *1597*, 179–193.

Yoshimura, Y., Taguchi, A., Tanigawa, S., Yatsuda, J., Kamba, T., Takahashi, S., Kurihara, H., Mukoyama, M., and Nishinakamura, R. (2019). Manipulation of nephron-patterning signals enables selective induction of podocytes from human pluripotent stem cells. J. Am. Soc. Nephrol. *30*, 304–321.